PHYSICAL REVIEW A VOLUME 47, NUMBER 5 MAY 1993

Experimental transition probabilities of intercombination transitions in Mg-like and Al-like ions of bromine

E. Träbert
Ruhr-Universität Bochum, Bochum, Germany

J. Suleiman, S. Cheng, H. G. Berry, R. W. Dunford, E. P. Kanter, and C. Kurtz
Argonne National Laboratory, Argonne, Illinois 60439

A. E. Livingston, K. W. Kukla, and F. G. Serpa
University of Notre Dame, Notre Dame, Indiana 46556

L. J. Curtis
The University of Toledo, Toledo, Ohio 43606

(Received 21 December 1992)

Time-resolved extreme ultraviolet spectra of foil-excited 120-MeV Br ions have been recorded, using a spectrometer equipped with a position-sensitive detector. The spectra near $\lambda=20-30$ nm were measured at times after excitation of up to 6 ns. Prominent in the delayed spectra were the long-lived decays of the intercombination transitions in the Mg-like Br^{23+} and Al-like Br^{22+} ions. The present paper reports on lifetime measurements for intercombination transitions in highly charged bromine ions using such a position-sensitive detector.

PACS number(s): 34.50.Fa, 32.30.Jc, 32.70.Fw

I. INTRODUCTION

Intercombination transitions in few-electron ions or in ions with few electrons outside closed shells have been studied in several atomic systems; summaries of such studies and their applications can be found in Refs. [1–3]. Beam-foil spectroscopy is presently the only method which allows measurements of the lifetimes of long-lived levels in highly charged ions [4]. In order to facilitate a comparison of experimental and theoretical results, most studies have concentrated on systems with few electrons outside closed shells. For the Mg I isoelectronic sequence, the experimental data are satisfactory up to $Z=30$ (Zn) [2,5] in comparison with theoretical results and from the consistency between intermediate-coupling amplitudes obtained independently from spectroscopic and from lifetime data [6–8]. The database for the Al sequence is much poorer [2], there being fewer experimental lifetime data, and none for the longest-lived component of the lowest quartet term, $3s3p^2\,{}^4P_{3/2}$. In the Si I sequence, such intermediate-Z measurements might also check the expected result [9] that, with increasing Z, the intercombination multiplet $3s^23p^2\,{}^3P-3s3p^3\,{}^5S^\circ$ will be quenched in favor of the $3s^23p3d$ level decays.

The production of higher ionic charges along an isoelectronic sequence using the ion-foil interaction requires higher ion beam energies to reach such charge states. The beam currents (and hence the expected signal rates) are likely to be less than those of lower-energy machines [2,10,11], encouraging the application of multichannel detectors [12–18]. The present paper reports on intercombination transitions in highly charged ions.

II. EXPERIMENT

The experiment was performed at Argonne National Laboratory using the ATLAS accelerator facility. A beam of 120-MeV ^{79}Br ions of 3–6 particle nA of current was directed through thin (2–10 μg/cm^2) carbon foils. The energy loss in these foils amounts to less than 2% [19] and thus is a minor correction for the present experiment. The ion energy chosen is close to optimum for the production of ions in the Mg-like charge state; the expected charge state distribution after passage through a sufficiently thick foil [20] also contains a major fraction of Al- and Na-like ions and a minor fraction of Si-like ions. For the 2 μg/cm^2 foil thickness, however, charge state equilibrium would not yet be reached [21].

The extreme ultraviolet radiation emitted by the foil-excited bromine ions was dispersed by a 600-l/mm ruled grating in a 2.2-m grazing-incidence spectrometer set at an angle of incidence of 84°. The detector consisted of a 25-mm microchannel plate with a resistive-anode position readout. The angle between the detector normal and the optic axis was about 60°, optimizing the detection efficiency. At each spectrometer setting, the width of the detector corresponded to a wavelength interval of about 10 nm. The signal was normalized to the beam charge collected in a Faraday cup.

III. RESULTS AND DISCUSSION

Spectra, with the foil positioned inside the field of view of the detection system, were recorded over the range $\lambda=14-55$ nm. A few known transitions within the $n=3$

shells of the bromine ions with 11–14 electrons served to wavelength calibrate the spectra [22–26]. Hydrogenic transitions ($n = 6 \rightarrow 7$, $7 \rightarrow 8$, $8 \rightarrow 9$) in Ne-, Na-, Mg-, and Al-like bromine were identified in the wavelength range 18–53 nm in the prompt spectra. The measured wavelengths of the dominant peaks of these transition complexes are all blueshifted (i.e., to shorter wavelengths) with respect to the Dirac values of the equivalent one-electron hydrogenic transitions. These wavelength shifts are consistent with the predicted wavelength corrections from a polarization model approximation for nonpenetrating high angular momentum Rydberg states. In addition, the spectra show some complicated structures associated with the Mg- and Al-like hydrogenic transitions resulting from the larger atomic core polarizabilities for these multivalence electron systems. However, the wavelength precision in the present measurements and the complexity of the prompt spectra precluded an accurate test of the predicted polarization corrections. The relative intensities of the observed hydrogenic transitions qualitatively confirmed the expected charge state distribution.

Before and after the run the detection system was also calibrated with a neon gas discharge source. This spectrum provides the wavelength calibration curve of the detector (at each spectrometer setting) and permits the interpolation of the wavelengths between in-beam calibration lines. Overlapping spectra helped in accounting for the nonuniformity of the efficiency across the detector, and this was taken into account in the interpretation of the spectral features observed. The wavelength calibration precision based on in-beam reference lines is ±0.03 nm for resolved lines in the center part of each individual spectrum where the nonlinearities of the detector are smallest. The precision is limited by the lack of identified neon lines below 30 nm. For weak lines not covered by the center of the plate, the uncertainties are substantially larger.

In order to record delayed spectra or decay curves, the foil could be displaced from the field of view of the detection system by up to about 10 cm, which corresponds to a flight time of 6 ns at our ion energy. This is equivalent to about three decay lengths for most of the long-lived levels studied here. In the spectral range of interest for the intercombination transitions, $\lambda = 20-30$ nm, 11–15 spectra at different foil positions were recorded at each of several detector positions resulting in overlapping spectra (Fig. 1). At each detector position the sequence of the predetermined foil positions was repeated a number of times and the spectra for a given foil position were summed. This fairly fast cyclic mode helped to reduce possible effects of foil deterioration on each data sample.

In the wavelength region of interest, five strong lines with notable intensities away from the foil were observed (for a sample spectrum, see Fig. 2). These were the $3s\,^2S_{1/2}-3p\,^2P^\circ_{1/2,3/2}$ resonance lines in the Na-like ion Br^{24+} (at $\lambda = 22.9228$ nm and 18.9621 nm, respectively [22]), the intercombination lines $3s^2\,^1S_0-3s3p\,^3P^\circ_1$ in the Mg-like ion Br^{23+} ($\lambda = 25.374$ nm [27]), the $3s^23p\,^2P^\circ_{3/2}-3s3p^2\,^4P_{5/2}$ line in the Al-like ion Br^{22+} ($\lambda = 26.035$ nm [28]) and a line near 20.6 nm which is assigned to the $3s^23p\,^2P^\circ_{3/2}-3s3p^2\,^2D_{5/2}$ transition in Br^{22+}. The first four of these lines also provide convenient wavelength references in the delayed spectra. The search for the weaker lines of the intercombination transition multiplets in the Al- and Si-like ions took advantage of the recording technique: The delayed spectra were summed to provide better statistical precision than that of each individual spectrum. For the decay curves, a given line in each individual spectrum was integrated over the full linewidth and the decay curve was constructed from the full integrated signal at each foil posi-

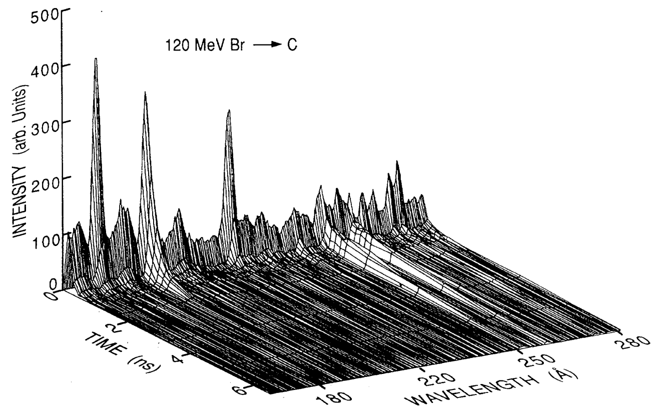

FIG. 1. Three-dimensional plot of spectra of bromine ions recorded at various foil positions. The presence of the decays of many short-lived levels in the spectra recorded close to the foil is evident; at longer times after excitation the few remaining lines are from the decays of long-lived intercombination transitions.

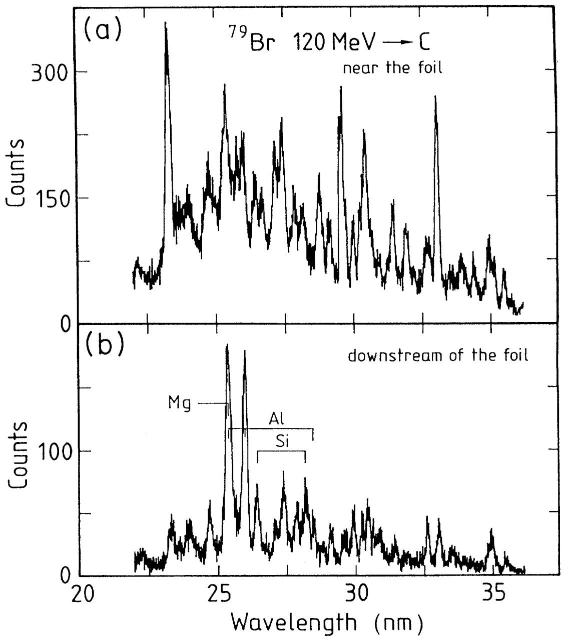

FIG. 2. Sample spectrum. (a) Sum of the spectra recorded near the foil, (b) sum of the spectra recorded away from the foil. The latter enhances the lines associated with decays of long-lived levels.

tion.

The decay curves were analyzed by least-squares fits to multiexponential functions plus a constant background attributed to detector dark counts and ion-beam-related background. This (low) background rate was directly measured with the foil positioned downbeam of the field of view of the detection system. For short-lived components, the shape of the detection window (field of view plus other corrections [29]) was introduced into the fitting procedure in order to reduce some of the ambiguities of multiexponential fitting and to fully exploit the time resolution available. The spectra recorded near the foil show a strong, nonuniform background. This background may consist of secondary-electron bremsstrahlung as well as radiation from the decays of short-lived, core-excited levels, possibly in various higher diffraction orders. The long-lived transitions can be clearly distinguished from these short-lived contaminants.

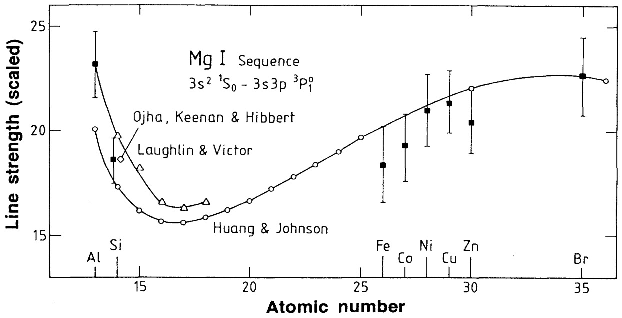

FIG. 3. Mg I sequence: Scaled line strength S as a function of nuclear charge (or atomic number). The quantity $(S/10^{-6}\zeta^2)$ is displayed, where ζ is the ionic core charge. The multiconfiguration relativistic random-phase approximation (MCRRPA) calculation extending to the Br ion is by Huang and Johnson [34], the low-Z theory by Laughlin and Victor [35] is based on a model-potential calculation. For discussions of theory and the result of a configuration-interaction calculation for $Z=14$ see also Refs. [38,39].

All decay curves suffered from blends with decays from short-lived levels. It was nevertheless straightforward to approximate the delayed components of the decay curves by one or two exponentials. Despite recent progress on the systematics of the dependences of the level population on the principal and angular momentum quantum numbers n and l (see [30,31]), the precision achievable by modeling these cascades in our system remains limited. At the present signal level and length of decay curves observed, slow yrast cascades (from levels of maximum l for a given value of n) can be taken into account by one slow exponential component (representing the manifold of slow cascades from very-high-lying hydrogenic levels) [32]; however, there are no criteria for an optimum choice of such a component, contributing to a small uncertainty in the evaluation. In the present case, where most of the lifetimes of interest are close to 2 ns, the starting value of the slow component was set in the range 4–8 ns. The upper limit is determined by the minimum signal which can be separated from a constant (beam-related plus detector dark count) background. In principle, a realistic background can be obtained from decay curves of the signal between spectral lines. However, because of the high, unresolved spectral density of lines near the foil, only the background level in the delayed spectra can be used in this manner. This is compatible with the assumption of a flat (constant) background. The results of our fits to the data are given in Table I. Figures 3, 4, and 5 show our lifetime results with the systematic trends for these intercombination transitions in the Mg I, Al I, and Si I isoelectronic sequences, respectively. References to work on other ions are found in Ref. [2].

Table I includes the longest-lived $3s3p^2\,^4P_J$ level in Al-like ions, $J=\frac{3}{2}$. The identification of this transition results from the clear signature of the shape of the decay

TABLE I. Wavelength and lifetime results.

		Wavelength (nm)		Lifetime (ns)	
Ion	Transition	Experiment [Ref.]	Theory [Ref.]	Experiment[a]	Theory [Ref.]
Br^{23+}	$3s^2\,^1S_0-3s3p\,^1P^\circ_1$	16.6805 [23]	16.535 [23]	0.053±0.03[b]	0.02 [47]
Br^{24+}	$3p\,^2P^\circ_{3/2}-3d\,^2D_{5/2}$	16.6772 [23]		same (blend)	0.038 [48]
Br^{24+}	$3s\,^2S_{1/2}-3p\,^2P^\circ_{3/2}$	18.9622 [22]	18.9625 [49]	0.10±0.03[b]	0.058 [48]
Br^{22+}	$3s^22p\,^2P^\circ_{3/2}-3s3p^2\,^2D_{5/2}$	20.58±0.03[a]	20.45 [36]	0.235±0.02	0.27 [36]
Br^{24+}	$3s\,^2s_{1/2}-3p\,^2P^\circ_{1/2}$	22.9223 [22]	22.9227 [47]	0.11±0.03[b]	0.091 [48]
				0.12±0.03	
Br^{23+}	$3s^2\,^1S_0-3s3p\,^3P^\circ_1$	25.3710 [23]	25.304 [23]	1.86±0.15	1.80 [34]
Br^{22+}	$3s^22p\,^2P^\circ_{1/2}-3s3p^2\,^4P_{1/2}$	25.56±0.03[a]	25.564 [36]	1.9±0.2	1.71 [36]
Br^{22+}	$3s^23p\,^2P^\circ_{3/2}-3s3p^2\,^4P_{5/2}$	26.01±0.03[a]	26.047 [36]	2.05±0.10	2.05 [36]
Br^{21+}	$3s^23p^2\,^3P_1-3s3p^3\,^5S^\circ_2$	26.49±0.05[a]	26.630 [37]		
		26.457 [33]		3±1	2.92 [37]
Br^{21+}	$3s^23p^2\,^3P_2-3s3p^3\,^5S^\circ_2$	28.47±0.1[a]	28.576 [37]		
		28.286 [33]			
Br^{22+}	$3s^23p\,^2P^\circ_{3/2}-3s3p^2\,^4P_{3/2}$	28.74±0.15[a]	28.556 [36]	12±5	12.5 [36]
		28.485 [28]			

[a] This work

[b] Fit with two exponential components

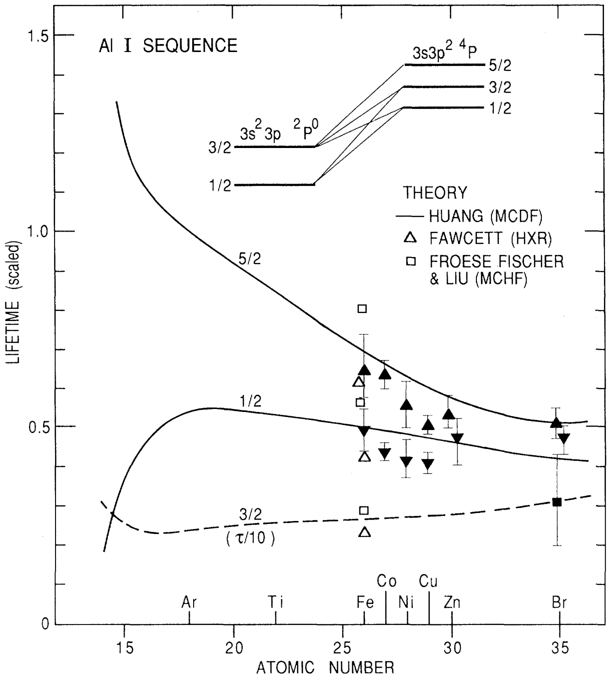

FIG. 4. Al I sequence: Scaled lifetime τ of the ^4P_J levels as a function of atomic number, Z. Theoretical values are taken from Refs. [40,41]. The vertical axis displays the quantity $[\tau(Z-10)^6\ \mathrm{s}^{-1}]$. The experimental data for the Br ion are from this work. Very recent work on Si^+ has been done by Calamai *et al.* [43] using an ion trap; these authors also discuss calculations done for very-low-charge-state ions.

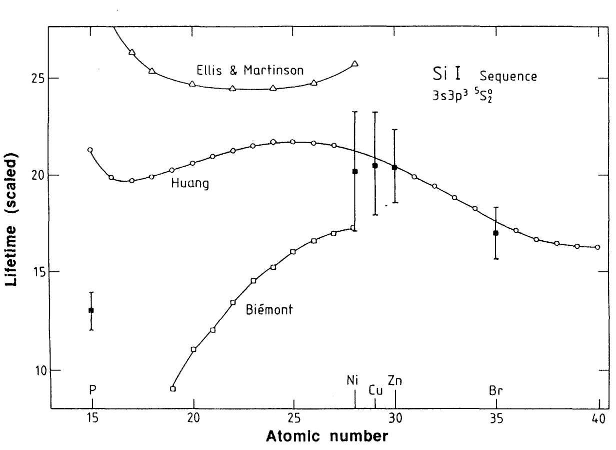

FIG. 5. Si I sequence: Lifetime [scaled as $\tau(Z-10)^7\ \mathrm{s}^{-1}$] of the $3s3p^3\ ^5S^\circ_2$ level. The only calculation for Br^{21+} is by Huang [37]. For references to calculations and experimental data at lower Z see Refs. [2] and Refs. [44–46] (calculations for P, S, and V). The result for P^+ is from Calamai, Han, and Parkinson [42], who used an ion trap. All other experimental data are from beam-foil measurements.

curve. The maximum foil displacement, however, corresponds to only about half the predicted length of this decay. At the observed signal level, this permitted the extraction of a lifetime value accurate to only approximately 40%. This particular decay will be more readily accessible in heavier ions, because of the favorable scaling of the transition probability with Z, and because of the scaling of the lifetime with the ion-beam velocity necessary to produce the proper ionization stage.

The observations of the intercombination lines in the $n=3$ shell of the Al- and Si-like ions confirm predictions of their wavelengths based on indirect evidence and on interpolations of isoelectronic trends. The present lifetime measurements agree with the predictions obtained by atomic structure programs based on the multiconfiguration relativistic random-phase approximation (MCRRPA) or multiconfiguration Dirac-Fock (MCDF) schemes (see Fig. 3). The present data represent a considerable extension of the previously available lifetime results towards higher nuclear charges.

ACKNOWLEDGMENTS

The production of stable ion beams by the ATLAS crew of operators is gratefully acknowledged. E.T. benefited from financial support by the Deutsche Forschungsgemeinschaft. This study was supported by the U. S. Department of Energy, Fundamental Interactions Branch, Office of Basic Energy Sciences, Division of Chemical Sciences, under Contracts No. W-31-109-ENG-38 (ANL), No. DE-FG02-92ER14283 (Notre Dame), and No. DE-FG05-88ER13958 (L.J.C., Toledo).

---

[1] I. Martinson and D. G. Ellis, Comments At. Mol. Phys. **16**, 21 (1985).
[2] E. Träbert, P. H. Heckmann, R. Hutton, and I. Martinson, J. Opt. Soc. Am. B **5**, 2173 (1988).
[3] D. G. Ellis, I. Martinson, and E. Träbert, Comments At. Mol. Phys. **22**, 241 (1989).
[4] L. J. Curtis and I. Martinson, Comments At. Mol. Phys. **24**, 213 (1990).
[5] E. Träbert, Phys. Scr. **41**, 675 (1990).
[6] L. J. Curtis, Phys. Rev. A **40**, 6958 (1989).
[7] L. J. Curtis, Z. B. Rudzikas, and D. G. Ellis, Phys. Rev. A **44**, 776 (1991).
[8] L. J. Curtis, J. Opt. Soc. Am. B **9**, 5 (1992).
[9] J. Bauche, C. Bauche-Arnoult, M. Klapisch, P. Mandelbaum, and J. -L. Schwob, J. Phys. B **20**, 1443 (1987).
[10] E. Träbert, Nucl. Instrum. Methods Phys. Res. Sect. B **31**, 233 (1988).
[11] E. Träbert, Nucl. Instrum. Methods Phys. Res. Sect. B **56/57**, 261 (1991).
[12] A. E. Livingston, S. J. Hinterlong, J. A. Poirier, R. DeSerio, and H. G. Berry, J. Phys. B **13**, L139 (1980).
[13] B. M. Johnson, K. W. Jones, D. C. Gregory, T. H. Kruse, and E. Träbert, Phys. Lett. **86A**, 285 (1981).
[14] E. Träbert, K. W. Jones, B. M. Johnson, D. C. Gregory, and T. H. Kruse, Phys. Lett. **87A**, 336 (1982).
[15] J. A. Demarest and R. L. Watson, Nucl. Instrum. Methods Phys. Res. Sect. B **24**, 296 (1987).
[16] S. Martin, J. P. Buchet, M. C. Buchet-Poulizac, A. Denis, J. Désesquelles, M. Druetta, J. P. Grandin, D. Hennecart, X. Husson, and D. Lecler, Europhys. Lett. **10**, 645 (1989).

[17] A. E. Livingston, F. G. Serpa, A. S. Zacarias, L. J. Curtis, H. G. Perry, and S. G. Blundell, Phys. Rev. A **44**, 7820 (1991).

[18] R. Büttner, B. Kraus, K. -H. Schartner, F. Folkmann, P. H. Mokler, and G. Möller, Z. Phys. D **22**, 693 (1992).

[19] L. C. Northcliffe and R. F. Schilling, Nucl. Data Tables A **7**, 233 (1970).

[20] R. O. Sayer, Rev. Phys. Appl. **12**, 1543 (1977).

[21] L. F. Pender and H. J. Hay, Phys. Rev. Lett. **50**, 1907 (1983).

[22] J. Reader, V. Kaufman, J. Sugar, J. O. Ekberg, U. Feldman, C. M. Brown, J. F. Seely, and W. L. Rowan, J. Opt. Soc. Am. B **4**, 1821 (1987).

[23] J. Sugar, V. Kaufman, and W. L. Rowan, J. Opt. Soc. Am. B **4**, 1927 (1987).

[24] J. Sugar, V. Kaufman, P. Indelicato, and W. L. Rowan, J. Opt. Soc. Am B **6**, 1437 (1989).

[25] J. Sugar, V. Kaufman, and W. L. Rowan, J. Opt. Soc. Am. B **5**, 2183 (1988).

[26] J. Sugar, V. Kaufman, and W. L. Rowan, J. Opt. Soc. Am. B **7**, 152 (1990).

[27] N. J. Peacock, M. F. Stamp, and J. D. Silver, Phys. Scr. **T8**, 10 (1984).

[28] C. Jupén, B. Denne, and I. Martinson, Phys. Scr. **41**, 669 (1990).

[29] E. Träbert, H. Winter, P. H. Heckmann, and H. V. Buttlar, Nucl. Instrum. Methods **135**, 353 (1976).

[30] H. -D. Betz, R. Höppler, R. Schramm, and W. Oswald, Nucl. Instrum. Methods Phys. Res. Sect. B **33**, 185 (1988).

[31] J. Kemmler, J. Burgdörfer, and C. O. Reinhold, Phys. Rev. A **44**, 2993 (1991).

[32] E. Träbert, Phys. Scr. **39**, 592 (1989).

[33] C. Jupén, I. Martinson, and B. Denne-Hinnov, Phys. Scr. **44**, 562 (1991).

[34] K.-N. Huang and W. R. Johnson, Nucl. Instrum. Methods Phys. Res. Sect. B **9**, 502 (1985).

[35] C. Laughlin and G. A. Victor, Astrophys. J. **234**, 407 (1979).

[36] K. -N. Huang, At. Data Nucl. Data Tables **34**, 1 (1986).

[37] K. -N. Huang, At. Data Nucl. Data Tables **32**, 503 (1985).

[38] A. Hibbert and A. C. Bailie, Phys. Scr. **45**, 565 (1992).

[39] P. C. Ojha, F. P. Keenan, and A. Hibbert, J. Phys. B **21**, L395 (1988).

[40] C. Froese Fischer and B. Liu, At. Data Nucl. Data Tables **34**, 261 (1986).

[41] B. C. Fawcett (private communication).

[42] A. G. Calamai, X. Han, and W. H. Parkinson, Phys. Rev. A **45**, 2716 (1992).

[43] A. G. Calamai, P. L. Smith, V. H. S. Kwong, and W. H. Parkinson (private communication).

[44] A. Hibbert, Phys. Scr. **38**, 37 (1988).

[45] T. Brage, G. Merkelis, and C. Froese Fischer (unpublished).

[46] D. G. Ellis, Phys. Scr. **40**, 12 (1989).

[47] L. J. Curtis, Phys. Scr. **43**, 137 (1991).

[48] C. E. Theodosiou and L. J. Curtis, Phys. Rev. A **38**, 4435 (1988).

[49] Y. K. Kim, D. H. Baik, P. Indelicato, and J. P. Desclaux, Phys. Rev. A **44**, 148 (1991).